

Depressed right ventricular systolic function in heart failure due to constrictive pericarditis

Veena Raizada^{1*} , Kimi Sato², Alaa Alashi³, Arnav Kumar⁴, Deborah Kwon⁵, Jay Ramchand⁵, Amy Dillenbeck⁵, Ross E. Zumwalt¹, Adarsh S. Vangala⁶, Tyler D. Earley⁷ and Allan Klein^{5*}

¹Department of Internal Medicine, University of New Mexico Health Sciences Center, 2211 Lomas Blvd, Albuquerque, NM 87131, USA; ²Department of Internal Medicine, Cardiology Division, University of Tsukuba, Tsukuba, Japan; ³Department of Internal Medicine, Texas Tech University Health Sciences Center, El Paso, TX, USA; ⁴Andreas Gruentzig Cardiovascular Center, Emory University School of Medicine, Atlanta, GA, USA; ⁵Center for the Diagnosis and Treatment of Pericardial Diseases, Section of Cardiovascular Imaging, Department of Cardiovascular Medicine, Heart, Vascular, and Thoracic Institute, Cleveland Clinic, 9500 Euclid Ave., Desk J1-5, Cleveland, OH 44195, USA; ⁶Department of Internal Medicine, Arizona Health Sciences Center, Tucson, AZ, USA; and ⁷Department of Internal Medicine, Samaritan Health Services, Corvallis, OR, USA

Abstract

Aims Heart failure in constrictive pericarditis (CP) is attributed to impaired biventricular diastolic filling. However, diseases that cause CP due to myocardial infiltration and fibrosis can also impair biventricular systolic function (sf) and contribute to heart failure. This study of patients with CP examined biventricular sf and the effect of myocardial infiltration by pericardial diseases and the resulting fibrosis on ventricular sf.

Methods and results Histopathologic examinations of right ventricular (RV) and left ventricular (LV) myocardia and pericardium were performed on three autopsied hearts of patients with pericardial diseases. Additionally, in 40 adults with clinical heart failure and 40 healthy adults (controls), sf of both ventricles was examined by echocardiography, including strain measurements, and biventricular diastolic filling and pulmonary artery pressures were assessed by cardiac catheterization. Cardiac histopathology indicated thickening of the pericardium with fibrosis, disease infiltrating the myocardium, greater infiltration of the RV than the LV, and an association of pericardial thickness with myocardial infiltrations. Functional analysis indicated that RVsf was impaired on all echo indices, including strain measurement, but LVsf was preserved.

Conclusions Diseases causing CP are not restricted to the pericardium but also infiltrate the biventricular myocardium and affect the thin-walled RV more than the thick-walled LV, resulting in depressed RVsf. The present results help explain clinical heart failure in the presence of restricted diastolic filling in CP. Depression of RVsf due to progression of fibrosis in the RV myocardium may increase the risk of delayed pericardiectomy.

Keywords Heart failure; Constrictive pericarditis; Right ventricle; Longitudinal strain

Received: 22 December 2020; Revised: 21 April 2021; Accepted: 30 April 2021

*Correspondence to: Veena Raizada, Department of Internal Medicine, University of New Mexico Health Sciences Center, 2211 Lomas Blvd, Albuquerque, NM 87131, USA.

Email: vraizada@salud.unm.edu

Allan Klein MD, Center for the Diagnosis and Treatment of Pericardial Diseases, Section of Cardiovascular Imaging, Department of Cardiovascular Medicine, Heart, Vascular, and Thoracic Institute, Cleveland Clinic, 9500 Euclid Ave., Desk J1-5, Cleveland, OH 44195, USA. Email: kleina@ccf.org

Introduction

Constrictive pericarditis (CP), which is characterized by encasement of the heart within a dense scarred pericardial sac, can cause heart failure due to external restriction of biventricular diastolic filling and elevated systemic and pulmonary venous pressures.¹ Patients with CP typically present with heart failure that manifests as ascites praecox, high jugular venous pressure, hepatomegaly, and pedal oedema,

with further complications of hepatic cirrhosis and protein-losing enteropathy. Heart failure in these patients is considered a progressive syndrome caused by a treatable extra-myocardial condition.^{1–3} The inflammatory and fibrotic processes associated with pericardial diseases that lead to pericardial fibrosis, scarring, and constriction can also infiltrate the ventricular walls^{4–6}; these affect the right ventricle (RV) more than the left ventricle (LV) because the RV has a thinner wall and a larger epicardial surface area in contact with the

diseased pericardial sac.^{7–11} Furthermore, histological studies of the myocardium in CP patients indicated increased deposition of collagen, fibrosis, and atrophy of myocytes, processes that may impair myocyte contractility.^{8–11} We therefore hypothesized that CP causes histopathological changes in the myocardium, with more severe changes in the RV than the LV and that these changes manifest as more severely impaired systolic function (sf) of the RV than the LV.

The study had two parts. Part I was a histopathologic examination of the myocardium and pericardium of the RV and LV from autopsy patients who had pericardial diseases with common aetiologies. Part II was an investigation of the sf of both ventricles using two-dimensional echocardiography (2DE), including measurements of longitudinal strain, in healthy controls and a group of patients with CP whose diagnoses were confirmed by cardiac catheterization.

Methods

Part I summarizes the histopathologic abnormalities of the pericardia and myocardia of the LVs and RVs from autopsies of three patients: a 59-year-old male with CP who died a few days following pericardiectomy; a 53-year-old female who had a breast malignancy and received radiation therapy; and a 41-year-old male who had malignant pericarditis. The pericardia and myocardia were stained with trichrome and haematoxylin and eosin and were then microscopically examined by an experienced pathologist. The slides were examined for collagen and fibrous connective tissue and inflammation involving the pericardia and myocardia, perimyocardial junctions and muscle bundles, and the subepicardial regions (*Figures 1–3*).

Part II consisted of 2DE measurements, including global longitudinal strain (GLS, ϵ), from 40 patients with heart failure due to CP (23 men, 17 women; mean age: 56 ± 14 years) from the database of the Cleveland Clinic (Cleveland, OH, USA). These patients were compared with 40 age-matched and gender-matched healthy control subjects. All measurements were conducted according to the guidelines of the American Society for Echocardiography.^{12,13} Data including GLS were analysed offline by the principal investigator (VR); this analysis was subsequently verified by two coinvestigators (KS and AA). Each value was obtained by averaging over 3 cycles. Diagnosis of CP was confirmed by intracardiac pressure measurements of the right atrium (RA), RV and LV, pulmonary artery, and pulmonary capillary wedge pressure using cardiac catheterization. The study protocol was approved by the institutional review board of the Cleveland Clinic, Cleveland.

Echocardiographic measurements

Pericardial thickness (millimetre) was measured using M-mode echocardiography, guided by 2DE in parasternal long-axis and subcostal views. To precisely measure pericardial thickness, images with clear separations between the parietal and visceral pericardia in diastole were selected.¹⁴ Measurements of RVsf included fractional area change (FAC), tricuspid annular plane systolic excursion (TAPSE), peak systolic velocity of tricuspid annulus (S'), and right ventricular index of myocardial performance (RIMP). RV wall thickness was measured at end diastole in subcostal and parasternal long-axis views. However, RV wall thickness could not be satisfactorily measured in all patients due to tethering and adhesions with the pericardium in both views. Inferior vena cava diameter was measured in subcostal views. Parasternal views of 2DE were used to derive LV end-diastolic and end-systolic internal dimensions, wall thickness, and mass. Apical views were used to estimate LV end-diastolic and end-systolic volumes and ejection fraction using Simpson's rule. The GLS of the LV and RV (LV ϵ and RV ϵ , respectively) in the apical four-chamber view was derived from the average strain of six segments of each ventricle.¹⁵

Statistical analysis

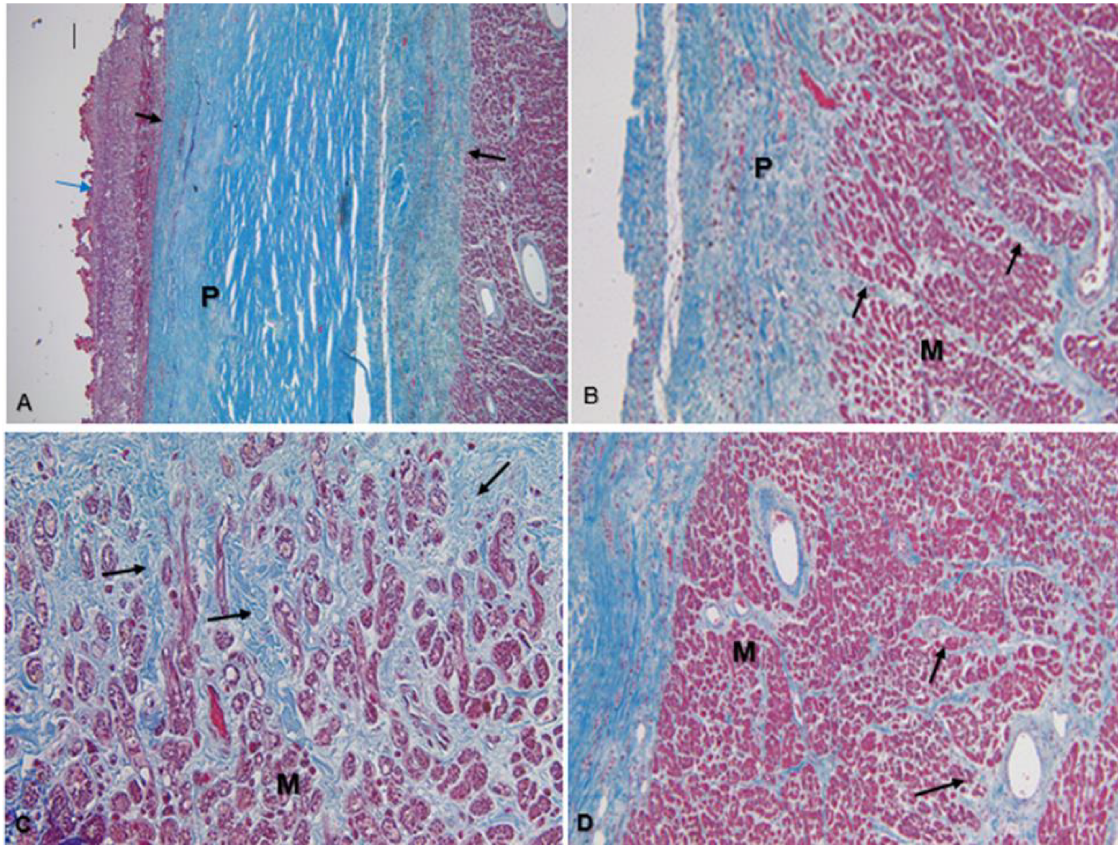
Continuous data are expressed as means \pm standard deviations when normally distributed and as medians and interquartile ranges (IQRs) when non-normally distributed. Categorical data are presented as absolute numbers and percentages. The unpaired *t*-test or McNemar's test was used to compare two groups, as appropriate. Spearman's correlation coefficient was used to assess correlations between echocardiographic and haemodynamic variables. To assess interobserver variability in strain measurements, two observers who were blinded to each other's measurements analysed 10 randomly selected datasets. Variability was assessed by intraclass correlation coefficients (ICCs) and presented as per cent variability. A *P* value below 0.05 was considered significant. All statistical analyses were performed using JMP Version 10.0 (SAS Institute Inc., Cary, NC, USA) and SPSS Version 25.0 (SPSS Inc., Chicago, IL, USA).

Results

Part I: Histopathologic examination of three autopsies

Photomicrographs (*Figures 1–3*) show the cardiac pathologies of the three autopsy patients. *Figure 1* (patient with CP) shows

Figure 1 Thick pericardial fibro-connective tissue with myocardial infiltration in post-inflammatory constrictive pericarditis. Photomicrographs of the right ventricle from a patient with post-inflammatory constrictive pericarditis. All photos show tissue stained with trichrome, which allows differentiation of fibrous connective tissue (stained blue) from exudate and myocardial cells (stained red). E, exudate; M, myocardium; P, pericardium. (A) Black arrows (4×) showing mature collagen and fibrous tissue. Dashed arrow shows inflammatory infiltration between the pericardium and adjacent tissue. (B) (10×) Junction of pericardial fibro-connective tissue and myocardium with black arrows showing strands of fibrous tissue between muscle bundles. (C) Black arrows (10×) showing increased fibrous tissue between myocardial muscle bundles. (D) (40×) Pericardial–myocardial junction with fibro-connective tissue surrounding many individual myocardial cells.



thick pericardial fibro-connective tissue and myocardium, with strands of fibrous tissue between the muscle bundles, and the presence of fibro-connective tissue surrounding many individual myocardial cells. *Figure 2* (patient with breast cancer who received radiation therapy) shows a thickened pericardium with fibrous tissue extending into the myocardium. *Figure 3* (patient with malignant pericarditis) shows the RV with a thickened epicardium and infiltration of large malignant cells that extended between the cardiac muscle fibres.

Part II: Echocardiographic and haemodynamic parameters in constrictive pericarditis patients and healthy controls

The aetiology of CP was idiopathic in 31 patients and was systemic disease (viral or bacterial infections) or radiation therapy in the other nine patients. The CP group had significantly greater pericardial thickness (6.0 ± 6.8 vs. 2.7 ± 0.30 mm, $P = 0.015$); however, there was no correlation

between pericardial thickness and RVsf parameters. The CP group had an FAC that was 12% lower, a TAPSE that was 57% lower, an S' that was 30% lower, and RIMP that was 35% greater (all $P < 0.001$). The two groups had similar RV linear internal dimensions, but the inferior vena cava was dilated in the CP group ($P < 0.001$). Both groups had normal LV size and LVsf, although all measures were lower in the CP group. The two groups had similar indexed LV mass (69 ± 13 vs. 64 ± 22 g/m², $P = 0.19$) (*Table 1*, *Figure 4*, top). The CP group had a significantly lower RVE compared with normal (-19.75 ± 3.22 vs. -25.32 ± 3.04 , $P < 0.001$), but the two groups had similar LVE (-19.42 ± 3.96 vs. -19.44 ± 0.72 , $P = 0.99$) (*Figure 4*, bottom).

Intracardiac pressures

Right heart pressures (RA, RV, pulmonary artery, and pulmonary capillary wedge pressure) were elevated in the CP group

Figure 2 Post-radiation constrictive pericarditis. Photomicrographs of the right ventricle from a patient with constrictive pericarditis who had undergone radiation therapy for breast cancer. (A) Black arrows [haematoxylin and eosin (H&E), 4×] showing thick fibrous pericarditis. (B) Black arrows (H&E, 10×) showing thickened pericardium with fibrous tissue adjacent to the myocardium. (C) Black arrows (H&E, 10×) showing thickened fibrous pericardium. (D) White arrows (H&E, 40×) showing the junction between the pericardium and myocardium with fibrous bands extending into the myocardium between cardiac muscle bundles.

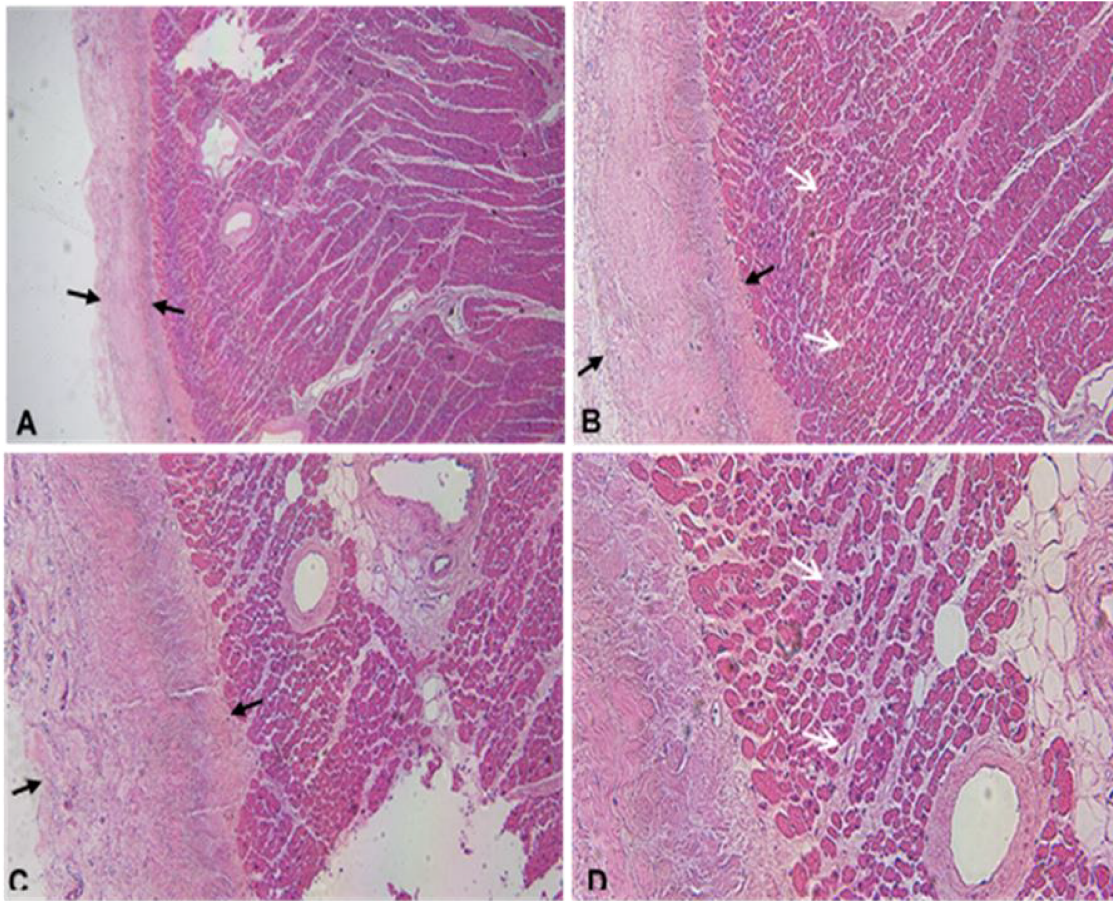


(Table 2), and simultaneous RV and LV pressure tracings showed a 'dip and plateau' pattern in diastolic pressure.

The interobserver variability accounted for 2% of the variability in LV strain and 4% of the variability in RV strain.

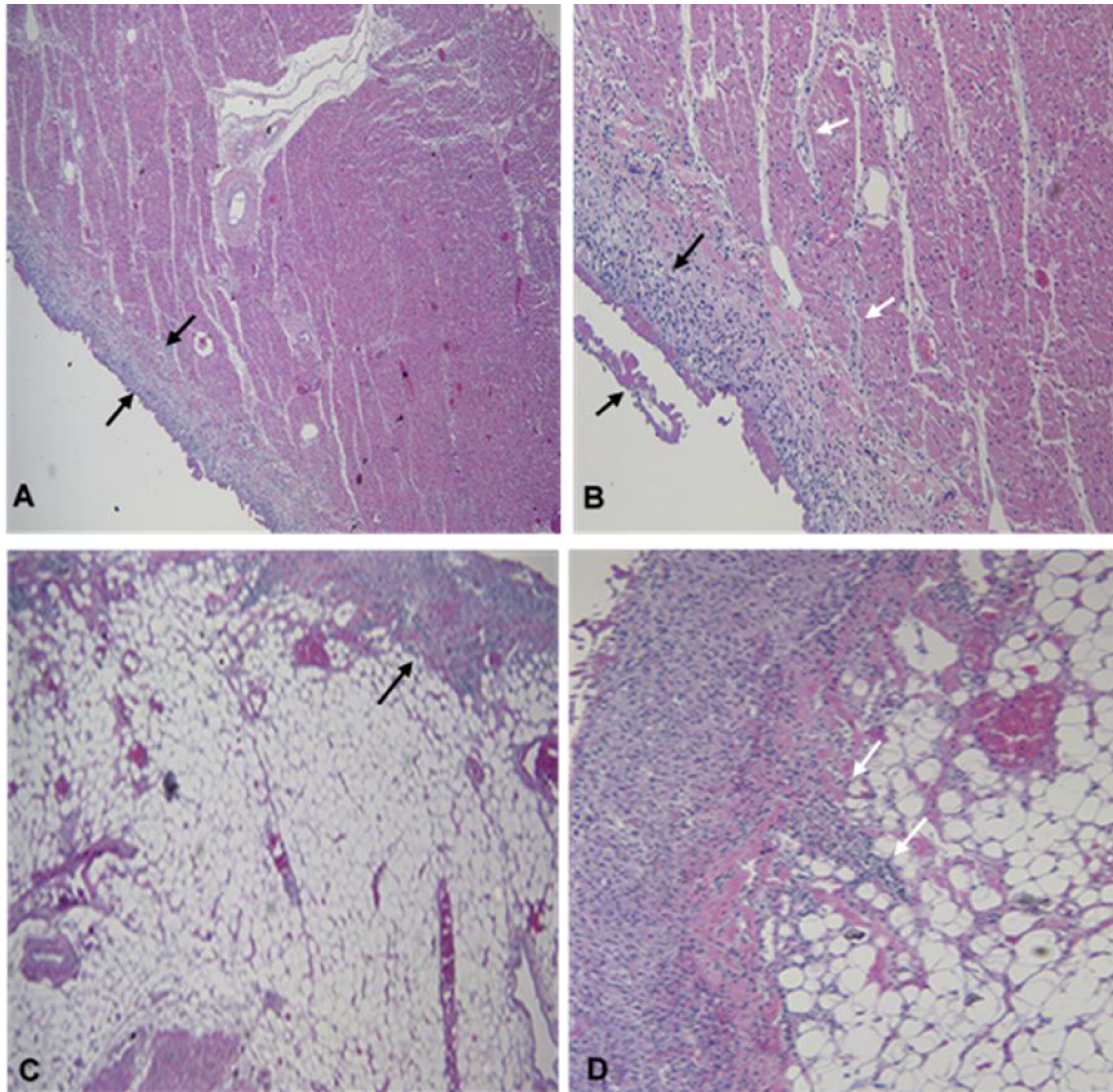
Variability data

Compared with normal population, CP patients showed significantly higher pericardial thickness (6.0 ± 6.8 vs. 2.7 ± 0.30 , $P = 0.015$). In CP patients, pericardial thickness was significantly correlated with RV dimension ($r = 0.45$, $P = 0.029$). While there was no correlation between pericardial thickness and RV geometry or function. The ICC for interobserver variability in GLS was 0.98 (IQR: 0.93–0.99) for LV and 0.95 (IQR: 0.85–0.98) for RV. The interobserver variability accounted for 5% of the variability in LV strain and 6% of the variability in RV strain. The ICC of intraobserver variability was 0.99 (IQR: 0.97–0.996) for LV strain and 0.98 (IQR: 0.94–0.99) for RV

Discussion

The patients included in this study had clinical symptoms of heart failure with characteristic clinical signs of CP. In all patients, cardiac catheterization demonstrated near equalization of diastolic pressures between the RV and LV and a preserved *x* wave with a prominent *y* descent due to impairment of biventricular diastolic filling resulting from pericardial constriction. The other major findings included (i) the presence of depressed RVsf and normal LVsf and increased pericardial thickness including adhesions with the epicardium, as determined by echocardiography, and (ii) cardiac pathology showing thick pericardium with fibrous tissue adjacent to the

Figure 3 Malignant pericarditis with myocardial infiltrates. Photomicrographs from a patient with malignant pericarditis. (A) Black arrows [haematoxylin and eosin (H&E), 4×] showing right ventricle with thickened epicardium, infiltration of large malignant cells, and associated inflammatory cells with fibrinous exudate on the surface. (B) Black arrows (H&E, 10×) showing right ventricle with thickened epicardium. White arrows indicate immature fibrous tissue extending between cardiac muscle fibres. (C) Black arrow (H&E, 4×) showing left ventricle with thickened epicardium and malignant infiltrate overlying subepicardial adipose tissue. (D) White arrows (H&E, 10×) showing the left ventricle epicardium with malignant infiltrate and inflammatory response extending into the subepicardial adipose tissue.



myocardium, abundant fibro-connective tissue along with cellular infiltrates extending to the myocardium, and excessive myocardial fibrosis, particularly of the RV wall.

We assessed RVsf using multiple echocardiographic indices according to the American Society for Echocardiography guidelines.^{12,13} Our evidence for a decreased RVsf was robust, as indicated by changes in four of the 2DE indices and a reduction in GLS. We found that, compared with healthy controls, CP patients showed a 12% to 68% change in all four of the 2DE indices and a 37% reduction in GLS, indicating significant impairment of RVsf in all patients. Interestingly, we found that RVsf was moderately to severely impaired by

traditional echo Doppler measurements as well as by reduction in GLS. Therefore, our experience in assessing RVsf in CP patients is not in line with prior studies of various diseases, which recommended that assessment of RVsf by traditional echo Doppler measurements should include measurement of GLS so as to improve the identification of patients who are at risk for clinical heart failure. Interestingly, LVsf was preserved in our CP patients, even though CP is characterized by encasement of both ventricles by a thick pericardial sac with excessive fibrosis. Our GLS measurements were also consistent with a lack of impairment of LVsf. The histopathologic changes in the pericardia and myocardia of

Table 1 Two-dimensional echocardiographic and Doppler characteristics of healthy controls and patients with constrictive pericarditis

Variable	Control (N = 40)	CP (N = 40)	P value
Right heart			
RV basal dimension (mm)	30 ± 3	30 ± 4	0.72
RV longitudinal dimension (mm)	66 ± 13	68 ± 13	0.59
RV mid-dimension (mm)	23 ± 8	28 ± 12	0.043
FAC%	55 ± 2	49 ± 5	<0.001
RV end-diastolic area (cm ²)	11.0 ± 1.4	13.0 ± 3.8	0.002
RV end-systolic area (cm ²)	4.9 ± 0.6	6.6 ± 2.1	<0.001
TAPSE (mm)	22 ± 2	14 ± 3	<0.001
S' (cm/s)	13 ± 1	10 ± 2	<0.001
RIMP	0.40 ± 0.04	0.62 ± 0.25	<0.001
Inferior vena cava (cm)	15 ± 0.2	31 ± 2.7	<0.001
Left heart			
LVIDd (mm)	45 ± 5	41 ± 7	0.007
LVIDs (mm)	29 ± 3	27 ± 5	0.036
EDV (mL)	97 ± 31	82 ± 31	0.029
ESV (mL)	35 ± 13	34 ± 15	0.65
EF (%)	64 ± 5	61 ± 6	0.011
IVSTd (mm)	8.7 ± 1.3	10.0 ± 1.9	0.001
PWTd (mm)	8.7 ± 1.4	9.6 ± 1.8	0.008
LVMI (g/m ²)	69 ± 13	64 ± 22	0.19

EDV, end-diastolic volume; EF, ejection fraction; ESV, end-systolic volume; FAC, fractional area change; IVSTd, interventricular septal thickness at end diastole; LVIDd, left ventricular internal diameter end diastole; LVIDs, left ventricular internal diameter end systole; LVMI, left ventricular mass index; PWTd, posterior wall thickness at end diastole; RIMP, right ventricular index of myocardial performance; RV, right ventricular; S', peak velocity of systolic mitral annular motion; TAPSE, tricuspid annular plane systolic excursion.

Data are expressed as means ± standard deviations.

the three autopsy cases point to the possible mechanisms responsible for depressed RVsf in CP. In particular, all three autopsy patients had changes in the pericardia and myocardia of both ventricles, but these changes were more extensive in the pericardium overlying the RV, as well as within the RV myocardium. The more extensive infiltration of the RV wall by inflammatory and malignant cells and fibrinous material from the thickened pericardium in our autopsy patients is consistent with our finding of impairment in the RVsf, and not of LVsf, in CP patients.

Mechanism(s) of reduced right ventricular systolic function

Our finding of reduced RVsf in CP appears related to the myocardial structural changes. There are three possible general causes of these structural changes. First, infectious and non-infectious pericardial diseases are characterized by inflammation that leads to subepicardial penetration of primary pericardial disease processes and extension into the myocardium, with replacement by fibrous connective tissue during healing.^{4-6,8-11} The molecular changes include release of pro-inflammatory and pro-fibrotic cytokines, and these promote the epithelial to mesenchymal transition, which is characterized by increased levels of connective tissue cytokines and increased extracellular matrix production and accumulation.^{4-6,16,17} Furthermore, pro-inflammatory cytokines inhibit protein synthesis, resulting in decreased levels of cardiac myofibrillar proteins and ultimately to reduced cardiac function.^{16,17}

Second, there is simultaneous involvement of the myocardium and pericardium in the same pathologic process, whether due to radiation therapy or collagen vascular diseases.⁴⁻⁶ This condition is not only restricted to the pericardium but also involves the myocardium and leads to perimyocarditis with subepicardial and myocardial inflammation, cellular infiltration, production of fibrinous exudate, and cell necrosis.¹⁶⁻¹⁸ Ultimately, there is fibrosis of the pericardium, and the fibrotic changes extend into the adjacent myocardium as shown in our autopsy cases.

The third cause of myocardial structural changes is myocardial ischaemia due to reduced coronary flow related to two main sources.^{19,20} The first source is diseases or therapies including radiation that induce or accelerate coronary artery disease, or invade the pericardium with subsequent fibrotic adhesions causing compression of the underlying coronary arteries. These pericardial diseases include fibrosis due to mediastinal irradiation or tumour infiltration, or following complicated open chest surgery, and systemic diseases including collagen vascular diseases and chronic renal failure. The second source is compression of coronary arteries from the outside by the contracting pericardial scar and the surrounding myocardial fibrosis, and restriction of diastolic coronary filling by excessively elevated biventricular diastolic filling pressures.²¹

Several observations indicate that the morphological and intracellular appearances of the myocytes in CP are due to ischaemia.^{19,20} Morphologically, populations of both large and small myocytes are observed (diameter, µm: normal = 14.5; large = 16.8; and small = 11.9). The former represent changes due to persistent ischaemic injury, and the latter

Figure 4 Depressed right ventricular (RV) systolic function in constrictive pericarditis (CP). (Upper) Comparison of four echocardiographic parameters, fractional area change (FAC), tricuspid annular plane systolic excursion (TAPSE), peak velocity of systolic mitral annular motion (S'), and right ventricular index of myocardial performance (RIMP), of RV in CP and C. FAC, TAPSE, and S' were lower and RIMP was higher in CP than in C ($P < 0.001$ for all). (Lower) The arrows on the global longitudinal strain of the right ventricle and left ventricle (RV ϵ and LV ϵ) curves represent average peak ϵ for the respective ventricle in patients with CP.

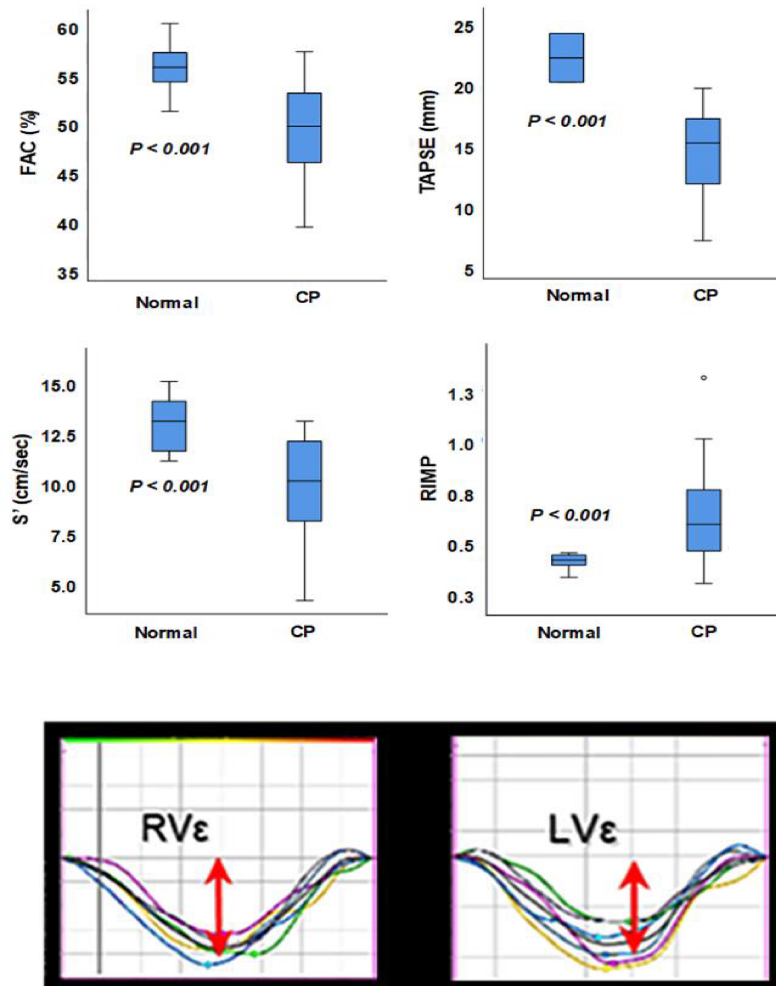


Table 2 Intracardiac right heart pressures in patients with constrictive pericarditis

Variable	Average \pm SD (mmHg)
RA mean	19 \pm 6
RV systolic	40 \pm 10
RV diastolic	20 \pm 6
PA systolic	38 \pm 10
PA mean	27 \pm 7
PCWP	21 \pm 6

PA, pulmonary artery; PCWP, pulmonary capillary wedge pressure; RA, right atrium; RV, right ventricle; SD, standard deviation.

represent early stages of ischaemia.¹⁹ However, some populations of the smaller cells may also be the result of disuse atrophy due to chronic cardiac compression by the thick and fibrosed pericardium.¹¹

Differential effects of pericardial disease on right ventricular and left ventricular structure

The different effects of CP on the RVsf and LVsf may be due to anatomical and/or physiological differences between the ventricles; regional variations in the severity of pericardial thickening; differences in the coverage of each ventricle by the pericardium; and differences in the anatomic location of the chamber in the chest cavity. The pericardial sac loosely covers the entire heart, but does not cover all chambers to the same extent.⁷

We attribute our observation, that CP had a greater effect on RVsf than LVsf, to the thinner RV wall and the unique anatomical position of the RV within the pericardial sac and chest cavity. As a result of this anatomical structure, there

is extensive contact between the diseased pericardial sac filled with exudate and the RV, especially along its diaphragmatic surface. Furthermore, the pericardium-to-RV contact is not limited to the epimyocardium, as chronic effusions are often accompanied by fibrous strands that span the pericardial space and infiltrate the entire thickness of the ventricular wall. Within the ventricular wall, fibrous connective tissue is present along with the pathologic material intermingling with myocardial fibres. This pathologic change within the RV myocardium contributes to impairment of the RVsf and in some cases also induces extrinsic compression of the coronary arteries, leading to myocardial ischaemia. Accordingly, the histopathological changes (cellular infiltrates, fibrous strands, and scarring) due to chronic pericardial disease are more extensive in the thin-walled RV than in the thick-walled LV, in agreement with what we observed in the three autopsied hearts (Figures 1–3). These histopathologic abnormalities of the RV wall and the increase in afterload due to pulmonary hypertension are the likely explanations of the reduced RVsf in our patients. On the other hand, our patients had preserved LVsf. These findings suggest that the pericardial involvement of both ventricles would affect the RV much more than the LV because of the much smaller thickness of the RV wall, and compared with LV, more extensive contact of the RV with the pericardium. Similar to the present study, Kusunose *et al.*²² found depressed RVsf in CP, but they also found depressed LVsf. Impaired LVsf in their study may be explained by the more severe myocardial fibrosis in these patients, because prior histopathological studies showed that extensive myocardial changes including ischaemia and myocyte atrophy, and fibrosis can occur due to longstanding and severe systemic diseases affecting the heart.^{8–11,16,17,23}

Finally, the present study and previous studies suggest that clinical heart failure in CP, although primarily due to restricted diastolic filling of both ventricles, can also represent impaired ventricular sf due to myocardial infiltration of pericardial disease. Accordingly, heart failure in CP, based on diagnostic features of diastolic heart failure with or without impaired ventricular sf, can be classified in three categories of increasing severity: (i) normal biventricular sf; (ii) impaired RVsf but normal LVsf; and (iii) impaired biventricular sf (Figure 5).

Limitations and strengths

Our group of CP patients had thickened pericardia, but pericardium thickness did not correlate with RVsf. This can be attributed to two factors that limited the accuracy of our measurements of pericardial thickness by transthoracic echocardiography: (i) collagen and fibrous tissue deposition between the pericardium and adjacent tissue, and between the pericardium and myocardium, and a thickened

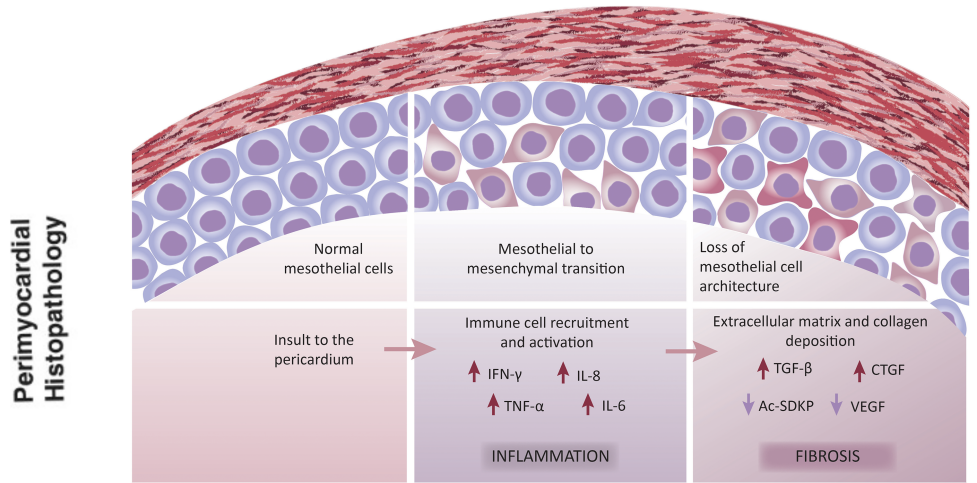
epicardium; and (ii) variations in operator technique, gain settings, and body habitus.

To improve the reliability of our measurements of global RVsf in RVs with unique geometry, we used multiple echocardiographic indices, including GLS, because each index measures a specific aspect of RVsf.^{12,13} A decreased global RVsf in CP represents decreased sf of the RV free wall because CP infiltrates the RV wall, not the interventricular septum. TAPSE and S' measurements assume that displacement of the basal region of the RV free wall represents sf of the entire RV; furthermore, these measurements are angle dependent. Nevertheless, the decreased TAPSE and S' values in the present study reliably represent impaired sf of the RV free wall. This is because the pericardial diseases that cause CP infiltrate the entire RV free wall and are not restricted to the basal region, although they do not infiltrate the interventricular septum. The percentage RV FAC, a measure of the decrease in RV diastolic to systolic area, correlates with RV ejection fraction determined by magnetic resonance imaging.²⁴ Although previous studies²¹ recommended using FAC to estimate RVsf, it does not represent the sf of the entire RV because it does not account for the contribution of the RV outflow tract. Furthermore, FAC measurements include function of the interventricular septum, which is unaffected in CP. On the other hand, RIMP estimates global RVsf, because a prolonged RIMP indicates reduced global RV contractility. Our CP patients had prolonged RIMP values, even though they had elevated RA pressure, which is known to reduce RIMP. Despite these limitations, considering these indices together, along with the decreased GLS, our findings are consistent with the interpretation CP leads to a decreased RVsf due to impaired function of the RV free wall.

Finally, our examinations of three autopsy cases provided important information about the pericardial and myocardial histopathological abnormalities in pericardial diseases—especially in the RV and LV. We had no echocardiographic or magnetic resonance imaging data on cardiac function in these autopsied hearts. However, our examinations provided new information about the pericardial and myocardial histopathological abnormalities caused by pericardial diseases.

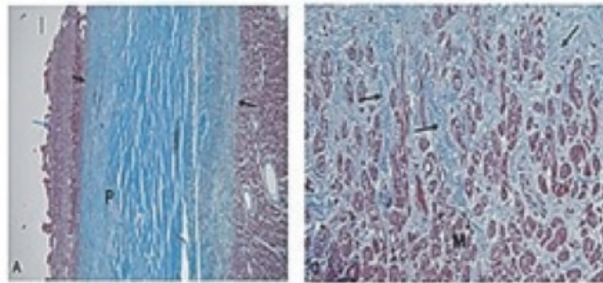
In conclusion, our study of 40 patients with CP and 40 healthy controls indicated the presence of depressed RVsf but preservation of LVsf in CP. The results of the echocardiographic examination of cardiac function and histopathologic investigation of myocardial tissues from autopsied hearts provide insights into the myocardial functional and structural changes that occur in CP. The cardiac structural changes in CP consisted of a thickened pericardium, fibrotic strands within the myocardium, and significantly denser fibrosis within the RV myocardium than the LV wall. The more abundant fibrosis in the RV compared with the LV appears to be due to the thin wall of the RV and the more extensive contact of its epicardium with the diseased pericardium. Myocardial fibrosis in which there is replacement of myocytes by fibrous tissue

Figure 5 Heart failure stages in constrictive pericarditis according to preserved versus impaired ventricular systolic function. (Top) Perimyocardial pathologic process leading to fibrosis and constrictive pericarditis (Ramasamy V et al. *World J Cardiol* 2018;10:87-96.)⁴; (Middle) Histopathologic changes leading to constrictive pericarditis (CP) in pericardium (left) and associated changes in the myocardium (right); and (bottom) stages of heart failure in CP: Stage 1, normal biventricular systolic function; Stage 2, reduced right ventricular systolic function (RVsf) with normal left ventricular systolic function (LVsf); and three categories of increasing severity: (i) normal biventricular systolic function; (ii) impaired RVsf but normal LVsf; and (iii) impaired biventricular systolic function.

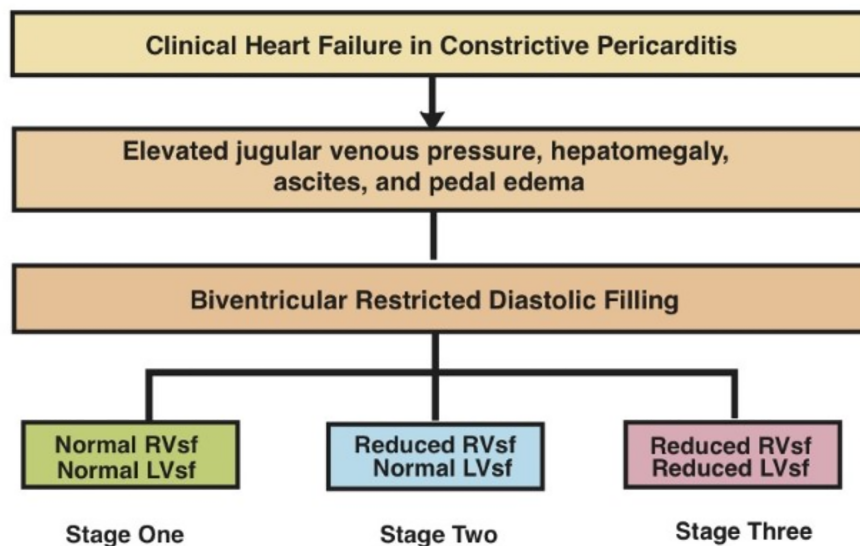


Molecular mediators involved in the inflammatory and fibrotic processes arising in constrictive pericarditis. Ac-SDKP: N-acetyl-seryl-aspartyl-lysyl-proline; TGF- β : Growth factor β ; TNF- α : Tumor necrosis factor- α ; CTGF: Connective tissue growth factor; IFN- γ : Interferon- γ ; VEGF: Vascular endothelial growth factor.

Perimyocardial Fibrotic Process



Categories of Cardiac Systolic Function in CP



and/or an increase of interstitial fibrous tissue with impairment of coronary blood supply is the likely cause of RVsf depression in patients with CP.

Clinical perspectives

Clinical heart failure in CP is traditionally attributed to restricted biventricular diastolic filling. However, pericardial diseases with myocardial incursions and consequent fibrosis can impair biventricular sf and affect the thin-walled RV more than the thick-walled LV. Accordingly, we propose three categories of heart failure in CP based on the type of ventricular function impairment: (i) biventricular diastolic function impairment with normal biventricular sf; (ii) biventricular diastolic function impairment with depressed RVsf and normal LVsf; and (iii) biventricular diastolic function impairment with depressed RV and LVsf. Consequently, pericardiectomy may not completely resolve heart failure in all patients with CP.

Translational outlook

A decline in diastolic function and sf of both ventricles in patients with CP affects their clinical course and prognosis. Therefore, myocardial infiltration by pericardial diseases

that impair cardiac function should be considered when testing cardiac function prior to pericardiectomy. Clinicians should consult with their patients and explain the expected level of post-operative recovery of cardiac function.

Acknowledgement

The authors thank Marie Phillip for her help with this research.

Conflict of interest

A. Klein MD discloses a research grant from Kiniksa and Sobi. The other authors disclose no relationships with industry and other entities.

Funding

There was no financial support including research grants and contracts involved in this research.

References

- Syed FF, Schaff HV, Oh JK. Constrictive pericarditis—a curable diastolic heart failure. *Nat Rev Cardiol* 2014; **11**: 530–544.
- Xanthopoulos A, Triposkiadis F, Starling RC. Heart failure with preserved ejection fraction: classification based upon phenotype is essential for diagnosis and treatment. *Trends Cardiovasc Med* 2018; **28**: 392–400.
- Yancy CW, Jessup M, Bozkurt B, Butler J, Casey DE Jr, Colvin MM, Drazner MH, Filippatos GS, Fonarow GC, Givertz MM, Hollenberg SM, Lindenfeld J, Masoudi FA, McBride PE, Peterson PN, Stevenson LW, Westlake C. 2017 ACC/AHA/HFSA focused update of the 2013 ACCF/AHA guideline for the management of heart failure: a report of the American College of Cardiology/American Heart Association Task Force on Clinical Practice Guidelines and the Heart Failure Society of America. *Circulation* 2017; **136**: e137–e161.
- Ramasamy V, Bongani M, Mayosi BM, Edward D, Sturrock E, Ntsekhe M. Established and novel pathophysiological mechanisms of pericardial injury and constrictive pericarditis. *World J Cardiol* 2018; **10**: 87–96.
- Chen MM, Lam A, Abraham JA, Schreiner GF, Joly AH. CTGF expression is induced by TGF- β in cardiac fibroblasts and cardiac myocytes: a potential role in heart fibrosis. *J Mol Cell Cardiol* 2000; **32**: 1805–1819.
- Yarnold J, Brotons MC. Pathogenetic mechanisms in radiation fibrosis. *Radiother Oncol* 2010; **97**: 149–161.
- Standring S. Heart. In Standring S., Gray H., eds. *Gray's Anatomy: The Anatomical Basis of Clinical Practice*, 40th ed, anniversary ed. Edinburgh: Churchill Livingstone/Elsevier; 2016. p 994–1023.
- Oh KY, Shimizu M, Edwards WD, Tazelaar HD, Danielson GK. Surgical pathology of the parietal pericardium: a study of 344 cases (1993–1999). *Cardiovasc Pathol* 2001; **10**: 157–168.
- Talwar KK, Narula JP, Chopra P. Myocarditis and myocardial interstitial fibrosis in constrictive pericarditis—an extended pathological spectrum. Constrictive pericarditis: a histopathological study of 91 cases. *Int J Cardiol* 1990; **29**: 241–243.
- Levine HD. Myocardial fibrosis in constrictive pericarditis. Electrocardiographic and pathologic observations. *Circulation* 1973; **48**: 1268–1281.
- Dines DE, Edwards JE, Burchell HB. Myocardial atrophy in constrictive pericarditis. *Proc Staff Meet Mayo Clin* 1958; **33**: 93–99.
- Rudski LG, Lai WW, Afilalo J, Hua L, Handschumacher MD, Krishnaswamy Chandrasekaran K, Solomon SD, Louie EK, Schiller NB. Guidelines for the echocardiographic assessment of the right heart in adults: a report from the American Society of Echocardiography endorsed by the European Association of Echocardiography, a registered branch of the European Society of Cardiology, and the Canadian Society of Echocardiography. *J Am Soc Echocardiogr* 2010; **23**: 685–713.
- Lang RM, Badano LP, Mor-Avi V, Afilalo J, Armstrong A, Ernande L, Flachskampf FA, Foster E, Goldstein SA, Kuznetsova T, Lancellotti P, Muraru D, Picard MH, Rietzschel ER, Rudski L, Spencer KT, Tsang W, Voigt JU. Recommendations for cardiac chamber quantification for echocardiography in adults. *J Am Soc Echocardiogr* 2015; **28**: 1–39.
- Klein AL, Abbara S, Agler DA, Appleton CP, Asher CR, Hoit B, Hung J, Garcia MJ, Kronzon I, Oh JK, Rodriguez ER, Schaff HV, Schoenhagen P, Tan CD, White RD. American Society of Echocardiography clinical recommendations for multimodality cardiovascular imaging of patients with pericardial disease: endorsed by the Society for Cardiovascular Magnetic Resonance and Society of

- Cardiovascular Computed Tomography. *J Am Soc Echocardiogr* 2013; **26**: 965–1012.
15. Lejeune S, Roy C, Ciocea V, Slimani A, de Meester C, Amzulescu M, Pasquet A, Vancraeynest D, Beauloye C, Vanoverschelde JL, Gerber BL, Pouleur AC. Right ventricular global longitudinal strain and outcomes in heart failure with preserved ejection fraction. *J Am Soc Echocardiogr* 2020; **33**: 973–984.e2.
 16. Valiente-Alandi I, Schafer AE, Blaxall BC. Extracellular matrix-mediated cellular communication in the heart. *J Mol Cell Cardiol* 2016; **91**: 228–237.
 17. Ehler E, Perriard JC. Cardiomyocyte cytoskeleton and myofibrillogenesis in healthy and diseased heart. *Heart Fail Rev* 2000; **5**: 259–269.
 18. Veinot JP, Edwards WD. Pathology of radiation-induced heart disease: a surgical and autopsy study of 27 cases. *Hum Pathol* 1996; **27**: 766–773.
 19. Gregory MA, Whitton ID, Cameron EW. Myocardial ischaemia in constrictive pericarditis—morphometric and electron microscopical study. *Br J Exp Pathol* 1984; **65**: 365–376.
 20. Navetta FI, Barber MJ, Gurbel PA, Moreadith RW, Bernstein R, Hlatky MA, Coleman RE, Bashore TM. Myocardial ischemia in constrictive pericarditis. *Am Heart J* 1988; **116**: 1107–1111.
 21. Moschowitz E. Pathogenesis of constrictive pericardium. *JAMA* 1953; **153**: 194–198.
 22. Kusunose K, Popović ZB, Motoki H, Alraies MC, Zurick AO, Bolen MA, Kwon DH, Flamm SD, Klein AL. Biventricular mechanics in constrictive pericarditis comparison with restrictive cardiomyopathy and impact of pericardiectomy. *Circ Cardiovasc Imaging* 2013; **6**: 399–406.
 23. Min T, Asp ML, Nishijima Y, Belury MA. Evidence for cardiac atrophic remodeling in cancer-induced cachexia in mice. *Int J Oncol* 2011; **39**: 1321–1326.
 24. Anavekar NS, Gerson D, Skali H, Kwong RY, Yucel EK, Solomon SD. Two-dimensional assessment of right ventricular function: an echocardiographic-MRI correlative study. *Echocardiography* 2007; **24**: 452–456.